

Hepatitis C virus proteins induce lipogenesis and defective triglyceride secretion in transgenic mice

Hervé Lerat ^{1*}, H  l  ne L. Kammoun ², Isabelle Hainault ², Emilie M  rour ¹, Martin R. Higgs ¹, C  line Callens ², Stanley M. Lemon ³, Fabienne Foufelle ², Jean-Michel Pawlotsky ^{1,4}

¹ *Institut Mondor de Recherche Biom  dicale INSERM : U955, Universit   Paris XII Val de Marne, IFR10, FR*

² *Centre de recherche des Cordeliers INSERM : U872, Universit   Pierre et Marie Curie - Paris VI, Universit   Paris Descartes, CRBM des Cordeliers 15, rue de l'ecole de medecine batiment E 75270 Paris cedex 06,FR*

³ *Institute of Human Infections and Immunity University of Texas Medical Branch, Galveston, Texas,US*

⁴ *Service de bact  riologie, virologie, hygi  ne Assistance publique - H  pitaux de Paris (AP-HP), H  pital Henri Mondor, Universit   Paris XII Val de Marne, FR*

* Correspondence should be addressed to: Herv   Lerat <herve.lerat@inserm.fr >

Abstract

Chronic hepatitis C virus (HCV) infection is associated with altered lipid metabolism and hepatocellular steatosis. Virus-induced steatosis is a cytopathic effect of HCV replication. The goal of this study was to examine the mechanisms underlying HCV-induced lipid metabolic defects in a transgenic mouse model expressing the full HCV protein repertoire at levels corresponding to the human infection. In this model, expression of the HCV full-length open reading frame was associated with hepatocellular steatosis and reduced plasma triglyceride levels. Triglyceride secretion was impaired while lipogenesis was activated. Increased lipogenic enzyme transcription resulted from activation at the maturation step and nuclear translocation of sterol regulatory element binding protein 1c (SREBP1c). No ER-stress marker was expressed at significantly higher levels in HCV transgenic mice than in their wild-type counterparts, suggesting that SREBP1c proteolytic cleavage was independent of ER stress. In conclusion, transgenic mice expressing the HCV full-length polyprotein at low, physiological levels, have decreased plasma triglyceride levels and develop hepatocellular steatosis in the same way as HCV-infected patients. In these mice, de novo triglyceride synthesis is induced by direct SREBP1c activation by one or several HCV proteins through induction of the lipogenic pathway, independently of ER stress, while triglyceride secretion is simultaneously reduced.

MESH Keywords Animals ; Blotting, Western ; Disease Models, Animal ; Endoplasmic Reticulum ; metabolism ; Fatty Liver ; blood ; etiology ; metabolism ; Hepacivirus ; genetics ; metabolism ; Hepatitis C ; blood ; complications ; metabolism ; Humans ; Lipogenesis ; physiology ; Liver ; metabolism ; pathology ; virology ; Male ; Mice ; Mice, Inbred C57BL ; Mice, Transgenic ; Reverse Transcriptase Polymerase Chain Reaction ; Sterol Regulatory Element Binding Protein 1 ; genetics ; metabolism ; Triglycerides ; blood ; secretion ; Viral Proteins ; genetics ; metabolism

Chronic hepatitis C virus (HCV) infection affects approximately 170 million individuals worldwide and is associated with chronic liver inflammation and fibrosis. Approximately 20% of patients develop cirrhosis, with a subsequent risk of lethal complications such as end-stage liver disease and hepatocellular carcinoma (1). Chronic HCV infection is now the leading indication for liver transplantation in industrialized countries. Chronic hepatitis C is curable in about 50% of cases with a combination of pegylated interferon- α and ribavirin (1). New drugs, and particularly specific inhibitors of HCV functions, are in preclinical and clinical development (2).

Chronic HCV infection is also associated with altered lipid metabolism, resulting in low serum cholesterol, triglyceride and betalipoprotein levels (3,4). These abnormalities generally resolve after viral eradication (3,5). Hepatocellular steatosis, i.e. excessive triglyceride accumulation within lipid droplets in the hepatocyte cytoplasm, is frequent in chronic hepatitis C (6). Steatosis may be due to metabolic disorders in patients with overweight, diabetes, dyslipidemia, and/or chronic alcohol consumption (metabolic steatosis). Steatosis may also be directly related to virus replication (virus-induced steatosis), and both forms may be present together. Metabolic steatosis behaves in a similar way as in HCV non infected patients with non alcoholic fatty liver disease or alcoholic liver disease, and appears to influence the outcome of chronic liver disease and undermine the effectiveness of antiviral therapy (7,8). Virus-induced steatosis is a cytopathic effect of HCV replication, but the precise underlying mechanisms are controversial. The influence of virus-induced steatosis on the outcome of liver disease and the response to therapy is unclear. Although HCV-induced steatosis is mostly seen in patients with HCV genotype 3a infection, in whom it correlates directly with the level of viral replication, cases have been reported with other genotypes (9,10). The reasons for these genotype differences are unclear. The level of virus expression required for excessive triglyceride accumulation in hepatocytes might be lower in genotype 3 HCV infection.

Viral interaction with host lipid metabolism appears to be essential for the HCV cell cycle. Indeed, HCV replication occurs in association with endoplasmic reticulum (ER)-derived membranes and lipid droplets, and HCV core and nonstructural 5A (NS5A) protein addressing to lipid storage organelles plays an important role (11–14). We recently showed that HCV core protein alters lipid droplet morphology (15). Whether or not these effects play a role in hepatocellular steatosis is unclear. However, HCV protein expression has

been shown to induce steatosis in transgenic mice. In particular, we have previously shown that expression of the full HCV protein repertoire at physiological levels triggers hepatocellular steatosis in C57BL/6 mice (16). HCV protein expression thus appears sufficient to induce hepatocellular steatosis, without the need for viral replication. HCV protein expression might: i) induce de novo triglyceride synthesis; ii) reduce cellular triglyceride excretion; iii) alter triglyceride oxidation; and/or (iv) increase triglyceride uptake from serum.

Sterol regulatory element binding proteins (SREBP) belong to the basic helix-loop-helix-leucine zipper family (bHLH/LZ) of transcription factors. They are synthesized as precursor proteins bound to the ER. The SREBP1c isoform is predominant in the liver and preferentially enhances the transcription of genes involved in fatty acid synthesis. Foreign protein synthesis inside host cells creates non specific stress that triggers the unfolded protein response (UPR). During the UPR, SREBP1c is matured by two successive cleavage steps and its transcription factor domain relocates to the nucleus, where it upregulates numerous genes involved in lipid synthesis and maturation. However, the effect of HCV proteins on these processes is largely unknown.

The goal of this study was to examine the mechanisms underlying HCV-induced lipid metabolic defects in a transgenic mouse model expressing the full HCV protein repertoire at levels corresponding to the human infection.

Experimental Procedures

Animals

Animal housing was conducted in accordance with the Direction des Services Vétérinaires, Ministère de l'Agriculture of France, with the European Communities Council Directive (86/609/EEC) and with the Federation of European Laboratory Animal Science Associations (FELASA) for the health monitoring recommendations. Eight- to nine-month-old C57BL/6 male mice transgenic for the HCV full-length open reading frame (FL-N/35 lineage) (16) were used in this study. Age-matched wild-type male littermates were used as controls. The animals were housed in a temperature-controlled environment with a 12h light/dark cycle and had free access to water and a regular diet (D04 from SAFE, Augy, France: 6.1% carbohydrate, 3.1% fat and 15.8% protein). All procedures conformed to official French guidelines for the care and use of experimental animals. After sacrifice by CO₂ intoxication, liver tissue fragments were either immediately snap-frozen in liquid nitrogen and stored at -80°C for analysis, or fixed overnight (approximately 16 h) in neutral buffered formalin before transfer to 70% ethanol and embedding in paraffin. Sections 4–5 µm thick were deparaffinized and stained with hematoxylin and eosin (H&E) for histological analysis.

Assessment of hepatic triglyceride and apolipoprotein content

Frozen tissue sections were stained with Oil-Red-O dye to identify neutral lipids. As previously described (17), serum triglycerides and apolipoprotein B (apoB) were quantified immediately before and 4 h after intraperitoneal injection of 30 mg of Triton WR 1339 (Tyloxapol, Sigma, Saint-Louis, Missouri) in 24h-fasted mice by using the Trinder Enzymatic method for triglycerides (Biotrol, Earth City, Missouri) and Kit 357 for apoB (Sigma).

Assessment of microsomal triglyceride transfer protein activity

Microsomal triglyceride transfer protein (MTP) activity was measured with a fluorometric assay (MTP kit, Roar Biomedical, New York, New York) that detects MTP-mediated transfer of neutral lipids in cell lysates or tissue homogenates, following the manufacturer's instructions. Liver samples were homogenized with a douncer in 15 mM Tris pH 7.4, 40 mM NaCl, 1 mM EDTA, plus protease inhibitors. MTP assay was performed by incubating 100 µg of liver protein homogenate (MTP source) with donor and acceptor solutions for 4 h at 37 °C. MTP activity was determined by measuring fluorescence at 465 nm (excitation) and 538 nm (emission).

Total RNA isolation and RT-qPCR

Total RNA was isolated from mouse livers as previously described (18) and 1 µg of RNA was reverse-transcribed with the Superscript II™ enzyme (Invitrogen, Carlsbad, California). Real-time quantitative PCR was performed with 25 ng of cDNA and 250 nM sense and antisense primers (Eurogentec, Seraing, Belgium) in a final reaction volume of 25 µl, using the qPCR Core Kit (Eurogentec) and the MyiQ real-time PCR detection system (Bio-Rad, Hercules, California). Specific primers were designed with Primer Express software (Table 1). The expression level of each studied gene was normalized to that of 18S ribosomal RNA by using the comparative C_T method.

XBP1 RT-PCR splicing assay

To analyze XBP1 mRNA splicing, 200 ng of cDNA was amplified with a pair of primers specific for the mouse XBP1 gene (sense: 5'-GGCCTTGTGTTGAGAACCAGGAG-3'; antisense: 5'-GAATGCCCAAAGGATATCAGACTC-3'). The PCR conditions are described in the Ron lab website (<http://saturn.med.nyu.edu/research/mp/ronlab/protocols.html>). PCR products were separated by electrophoresis on 2.5% agarose gels and visualized by ethidium bromide staining.

Preparation of cytoplasmic, microsomal and nuclear extracts and immunoblot analysis

Nuclear and cytoplasmic extracts were prepared from livers of wild-type and transgenic mice by using the NE-PER Nuclear and Cytoplasmic Extraction Reagent kit (Pierce Biotechnology, Rockford, Illinois), following the manufacturer's instructions. For microsomal extracts, mouse liver was homogenized in sucrose buffer (0.25 M sucrose, 10 mM Hepes, and 3 mM MgCl₂ supplemented with protease inhibitors, phenylmethylsulfonyl fluoride (1 mM), benzamide (1 mM), DTT (1 mM), leupeptin (2 µg/ml), and aprotinin (2 µg/ml)). The homogenate was centrifuged (500 g for 5 min at 4°C), and the supernatant was centrifuged again at 100,000 g for 45 min at 4°C to obtain microsomes.

The protein concentration was measured in the extracts by means of the Bradford method (Bio-Rad) with bovine serum albumin as standard. Proteins (20–70 µg) were separated by SDS-PAGE and transferred to nitrocellulose membranes (GE Healthcare, Chalfont St Giles, United Kingdom). The following primary antibodies were used: mouse monoclonal antibodies against SREBP1 clone 2A4 (Thermo Fisher Scientific, Waltham, Massachusetts), activating transcription factor 6 (ATF6) (Imgenex, San Diego, California), and X-box binding protein 1 (XBP1) (Prosci Inc., Poway, California); rat polyclonal antibodies against immunoglobulin heavy chain-binding protein (BiP)/glucose-regulated protein 78 (GRP78); and rabbit polyclonal antibodies against phosphoprotein kinase-like endoplasmic reticulum kinase (PERK) (Santa Cruz Biotechnology, Santa Cruz, California), and phospho-(Ser51)-eukaryotic initiation factor 2α (eIF2α), total Akt/protein kinase B (PKB) and eIF2α (Cell Signaling Technology, Beverly, Massachusetts). The membranes were incubated with the corresponding secondary antibodies coupled to peroxidase. Protein was quantified with the ECL Plus or Advance detection kit (GE Healthcare). A polyclonal mouse lamin A/C antibody (BD Biosciences, Franklin Lakes, New Jersey), calnexin and β-actin were used as loading controls for nuclear extracts, microsomal fractions and total lysates, respectively.

Statistical analysis

Results are expressed as means ± standard error of the mean. The Fisher-Yates Terry or Mann-Whitney non parametric rank tests were used, as appropriate. Quantitative results are presented as box plots (median and 95th percentiles).

RESULTS

Expression of the HCV full-length open reading frame is associated with hepatocellular steatosis and reduced plasma triglyceride concentrations in transgenic mice

Steatosis was scored after hematoxylin-eosin and Oil-red-O staining of liver tissues. Steatosis was considered absent, mild, moderate and severe when respectively 0%, <30%, 30–60% and >60% of hepatocytes were positively stained. Although C57Bl6 mice have a natural propensity to develop liver steatosis (19), moderate to severe hepatocellular steatosis was more frequent in transgenic mice than in controls (78% vs 29%, $p < 0.01$; Figure 1). In addition, plasma triglyceride levels were moderately but significantly lower in transgenic mice than in controls (0.77 ± 0.04 vs 0.86 ± 0.04 g/L, $p < 0.01$; Figure 2A, left).

Triglyceride secretion is impaired in mice transgenic for the HCV full-length open reading frame

Triglycerides are secreted from liver cells as very-low-density lipoprotein (VLDL) particles. Hepatic VLDL secretion was assessed in fasted mice by measuring the increase in plasma triglyceride and apoB levels after lipoprotein lipase inhibition by Triton WR 1339. As shown in Figure 2A, Triton treatment substantially increased the plasma triglyceride level. Plasma triglyceride levels were about 30% lower in transgenic mice than in controls (7.7 ± 0.4 vs 10.0 ± 0.5 g/L, $p < 0.002$), pointing to defective VLDL secretion (Figure 2A). This was confirmed by the significantly lower plasma level of apoB (a protein mainly present in VLDL and LDL) in transgenic mice than in controls after Triton treatment (2.5 ± 0.2 vs 3.7 ± 0.3 g/L, $p < 0.001$; Figure 2A).

MTP plays a key role in cotranslocational lipidation of apoB as it enters the ER lumen (thus preventing apoB degradation) and participates in the conversion of a precursor particle to VLDL by the addition of bulk triglycerides. As shown in Figure 2B, MTP activity was significantly lower in crude liver extracts from transgenic mice than from controls ($p < 0.05$), confirming the impaired triglyceride excretion.

Lipogenesis is activated in mice transgenic for the HCV full-length open reading frame

In order to determine whether the lipogenic pathway is activated in HCV transgenic mice, hepatic transcriptional levels of genes coding for various enzymes involved in lipogenesis were compared with values in non transgenic controls. These genes included ATP citrate-lyase (ACL), which produces acetyl-CoA, the substrate of fatty acid synthase (FAS); acetyl-CoA carboxylase (ACC) and FAS, which catalyze fatty acid synthesis; malic enzyme (ME), which generates nicotinamide adenine dinucleotide phosphate (NADPH), a cofactor of FAS; and hepatic stearoyl-CoA desaturase 1 (SCD1), a protein involved in fatty acid processing. Transcript levels of all these enzymes were higher in transgenic mice than in controls, as measured by RTqPCR (Figure 3A). The difference was statistically significant for ACL, FAS and SCD1 (fold increase compared to the mean values in non transgenic animals: 2.2 ± 0.6 , $p = 0.01$; 2.9 ± 0.7 , $p = 0.02$; and 2.0 ± 0.4 , $p = 0.02$, respectively), while a trend was observed for ACC and ME. FAS protein expression, quantified by western blotting of mouse liver extracts, was significantly higher in the liver of transgenic mice than in controls (Figure 3B). Together, these results suggest that the lipogenic pathway is activated in the liver of transgenic mice expressing the HCV full-length open reading frame.

SREBP1c is activated in mice transgenic for the HCV full-length open reading frame

Lipogenic enzymes are transcriptionally regulated by insulin and glucose through two transcription factors in the liver, namely SREBP1c and carbohydrate response element-binding protein (ChREBP). The SREBP1c precursor resides in the hepatocyte ER. Its activation involves two proteolytic cleavage steps which generate the mature form of the protein. The mature SREBP1c protein then migrates to the nucleus, where it activates the transcription of major genes involved in fatty acid synthesis. Nuclear and microsomal protein fractions were purified from liver extracts of transgenic and non transgenic animals, and SREBP1c levels were assessed by western blotting. Lamin A/C and calnexin served as loading controls for the nuclei and microsomes, respectively. As shown in figure 4A , microsomal fractions from transgenic and non transgenic animals contained similar amounts of SREBP1c precursor. In contrast, mature cleaved SREBP1c was substantially more abundant in nuclear extracts from transgenic animals than from controls (figure 4A), suggesting that increased lipogenic enzyme transcription in HCV transgenic mice results from activation and nuclear translocation of SREBP1c. The expression of ChREBP, a transcription factor involved in the activation of glycolytic and lipogenic genes, was not modulated by the HCV transgene (Figure 4A).

As shown in Figure 4B , the level of SREBP1c mRNA was slightly but not significantly higher in the liver of transgenic mice than in controls (fold increase compared to the mean control value: 1.3 ± 0.2 vs 1.0 ± 0.1 , $p=0.39$), suggesting that SREBP1c activation by HCV proteins occurs at the maturation step rather than through gene activation. Similarly, the expression of ChREBP transcripts was not modulated by the HCV transgene (Figure 4B).

ER stress is not induced in mice transgenic for the HCV full-length open reading frame

Eukaryotic cells respond to the stress due to ER accumulation of misfolded, unfolded or foreign proteins, including viral proteins, by activating a signalling pathway known as the UPR that induces temporary translational inhibition followed by upregulation of ER chaperones. ATF6, inositol-requiring element 1 (IRE1) and PERK are ER-resident transmembrane proteins bound to GRP78 (BiP). In UPR conditions they are released from GRP78 and activated. As HCV proteins are synthesized on ER membranes and remain closely associated with ER-derived membranous webs, we examined whether HCV protein expression could trigger an unfolded protein response in HCV transgenic mice.

We first measured GRP78 mRNA levels. As shown in Figure 5A , no significant difference was found between transgenic and non transgenic mice. IRE1 release from GRP78 activates IRE1 RNase activity and initiates mRNA splicing of XBP1, thus generating a spliced mRNA encoding a transcription factor that activates UPR target genes. We screened total RNA extracts from transgenic and non transgenic livers for spliced XBP1 mRNA by means of RT-PCR and observed no modulation of XBP1 splicing by the HCV transgene (Figure 5B).

PERK release from GRP78 induces PERK autophosphorylation and activation. Activated PERK (P-PERK) in turn phosphorylates eIF2 α , thereby reducing mRNA translation initiation. We measured phosphorylated PERK and eIF2 α by western blotting with specific antibodies, normalizing the results to the respective total amounts of the two proteins. As shown in Figures 5C and 5D , respectively, we found no difference in the levels of phosphorylated PERK and eIF2 α between transgenic and non transgenic animals.

Protein disulfide isomerase (PDI) is another chaperone involved in the ER-associated degradation (ERAD) pathway. ER degradation-enhancing mannosidase-like proteins (EDEMs) target UPR-inducing proteins and trigger their degradation. As shown in Figure 5E , quantitative RT-PCR revealed no significant differences in EDEM or PDI mRNA levels between HCV transgenic and non transgenic mice. C/EBP homologous protein (CHOP), also known as growth arrest- and DNA damage-inducible gene 153 (GADD153), is a component of the ER stress-mediated apoptosis pathway. TRB3 is induced by ER stress downstream of CHOP and was recently identified as a potential pro-apoptotic protein that can modulate the Akt/PKB-dependent signaling pathway. As shown in Figure 5F , CHOP and TRB3 expression levels did not differ between HCV transgenic and non transgenic mice, although there was a trend towards higher expression of CHOP transcripts in transgenic mice ($p < 0.06$).

Thus, none of the ER-stress markers tested here was expressed at significantly higher levels in HCV transgenic mice than in their wild-type counterparts. This suggests that SREBP1c proteolytic cleavage in transgenic mice expressing the HCV full-length open reading frame is independent of ER stress.

DISCUSSION

The mechanisms by which chronic HCV infection perturbs lipid metabolism are poorly understood. Intracellular virion production appears to use metabolic pathways involved in lipid metabolism (11 –15). Chronically HCV-infected patients often have low plasma cholesterol, triglyceride and betalipoprotein levels (3 ,20). In addition, virus-induced steatosis appears to be a direct cytopathic lesion

induced preferentially but not exclusively by genotype 3a HCV (21 ,22). A direct role of HCV is supported by the disappearance of these abnormalities when the infection is cured by antiviral therapy, and by their reappearance after HCV reinfection of the donor liver in HCV-infected transplant recipients (23 –25). The precise role of HCV protein expression in these phenomena is unclear.

The transgenic mice used here, which expresses the HCV full-length open reading frame, are a particularly relevant model for studying HCV protein-induced abnormalities, as all HCV proteins are produced at the same time at physiological levels, without virus production (16 ,26 –28). We have previously reported that two lineages of transgenic mice expressing the HCV full-length open reading frame develop more frequent and more severe hepatocellular steatosis than their non transgenic littermates (16). In the present study, chronic expression of the entire panel of HCV proteins in mice receiving a normal diet was associated with lower plasma triglyceride levels and with mediovesicular steatosis preferentially located in the central vein area, exactly as in human HCV infection (29 ,30).

Several mutually non exclusive mechanisms could theoretically explain these observations. HCV protein expression could i) induce de novo triglyceride synthesis; ii) reduce cellular triglyceride secretion; iii) alter triglyceride degradation; and/or iv) increase triglyceride uptake from serum. Here we tested the first two hypotheses in transgenic mice expressing the HCV full-length open reading frame. Taken together, our results suggest that HCV protein expression induces de novo triglyceride secretion independently of ER stress, and that it also reduces triglyceride secretion in this model.

Triglyceride synthesis from acetyl-CoA is a complex multistep process that includes lipogenesis, desaturation, elongation and esterification. These steps are catalyzed by different enzymes, expression of which was higher in the transgenic mice expressing the HCV full-length open reading frame than in non transgenic controls (Figure 3A). These findings suggest that de novo triglyceride synthesis induced by lipogenic pathway activation could at least partly explain the intracytoplasmic triglyceride accumulation observed in hepatocytes expressing HCV proteins. FAS also plays a central role in triglyceride synthesis. The increased FAS expression observed here in vivo, at both the mRNA and protein levels, is in keeping with recent results obtained with cellular models. Indeed, FAS has been shown to be upregulated in Huh-7 cells after transient expression of HCV core protein, after transfection with a full-length genome genotype 1b HCV replicon, and during infection by genotype 2a JFH1 virus (31 ,32). In addition, a Tet-regulated HeLa cell model stably expressing the HCV core protein has been developed (Li K, Lemon SM, unpublished). Core expression in this model was associated with microvesicular steatosis. Importantly, core protein expression did not increase lipid uptake in HeLa cells, which do not express MTP.

FAS expression is mainly regulated at the transcriptional level by SREBP1. FAS-SREBP1 pathway alteration has been shown to be associated with steatosis in vivo (33). We observed more mature SREBP1c in the nucleus of HCV transgenic mice than in non transgenic controls, possibly explaining the enhanced FAS mRNA expression in the transgenic mice. This is in keeping with the recent report that SREBP1c proteolytic cleavage is induced by JFH1 infection in Huh-7 cells (34). Likewise, a recent study comparing liver biopsy specimens from HCV-infected and uninfected patients showed no difference in hepatic SREBP1c mRNA levels, but SREBP1c protein levels were not studied (35). A role of HCV core, NS2 and NS4B proteins in SREBP1c proteolytic cleavage has been suggested, based on transient over-expression of sequences derived from different HCV genotypes (34 ,36 ,37). However, the viral protein(s) responsible for SREBP1c activation remain to be identified. Finally, contrary to SREBP1c, ChREBP, another potent regulator of FAS expression at the transcriptional level (38), was not involved in lipogenic pathway activation in our HCV transgenic mice.

SREBP-1c is a potent negative regulator of MTP expression (39). HCV protein activation of SREBP1c could thus down-regulate MTP activity, thereby explaining the decreased MTP activity that we observed in transgenic mice expressing the HCV full-length open reading frame. Reduced MTP activity could in turn be responsible for the defective VLDL secretion which, in combination with increased triglyceride synthesis, participates in hepatocyte triglyceride accumulation. It is noteworthy in this respect that reduced plasma MTP activity has also been reported in HCV-infected patients (40). Transgenic mice overexpressing HCV core protein also show reduced MTP activity (17), but MTP mRNA levels and activity are also reduced in the HCV subgenomic replicon model, which lacks HCV core protein (41).

Before concluding that de novo triglyceride synthesis mediated by enhanced FAS expression results from direct SREBP1c activation by HCV protein(s), it was important to eliminate a potential role of viral protein-induced ER stress. The unfolded protein response is triggered by the accumulation of unfolded, misfolded or foreign proteins within the ER. Thus, HCV protein expression and accumulation in transgenic hepatocytes could trigger ER stress, triggering non specific SREBP1c cleavage and activation. We therefore studied the three principal ER stress pathways, driven by PERK, ATF6 and IRE1, under the control of GRP78 (or BiP). None was found to be activated in transgenic hepatocytes: GRP78 expression, PERK and eIF2 α phosphorylation, and XBP-1 mRNA splicing were similar in HCV transgenic and non transgenic livers. These findings appear to conflict with previous reports. Indeed, ectopic expression of HCV envelope glycoproteins E1 and E2 has been reported to increase GRP78 expression (42). However, in these experiments, a large proportion of E1 and E2 proteins were trapped in the ER as aggregates, a phenomenon that does not occur during natural infection. Likewise, GRP78 expression has been reported to be induced in the replicon system, a replicative model based on Huh-7 cells. However, GRP78 induction was three times higher than in the same cells expressing HCV nonstructural proteins in the absence of replication, and HCV replication contributed to stimulating ER chaperone expression (43). Finally, the E2 envelope glycoprotein has been reported to bind PERK as a

pseudosubstrate, to inhibit its autophosphorylation, and to sequester it from its substrate eIF2 α , potentially masking downstream ER stress events (44). However, high E2 expression was required for this inhibition to occur. In addition, The FL-N/35 lineage is characterized by its very low level of HCV protein expression. Indeed, we were only able to demonstrate transgene expression within the mouse liver by using very sensitive immunochemical methods (26). Therefore, our findings conclusively show that HCV protein expression stimulates triglyceride synthesis independently of non specific ER stress activation.

In conclusion, transgenic mice expressing the HCV full-length polyprotein at low, physiological levels, have decreased plasma triglyceride levels and develop hepatocellular steatosis in the same way as HCV-infected patients. In these transgenic mice, de novo triglyceride synthesis is induced by direct SREBP1c activation by one or several HCV proteins through induction of the lipogenic pathway, independently of ER stress, while triglyceride secretion is simultaneously reduced. The HCV protein(s) responsible for these perturbations of lipid metabolism remain to be identified, along with the underlying molecular mechanisms.

Acknowledgements:

(HL) was supported by INSERM (Young Investigator Program), a grant from the Agence Nationale de Recherche sur le SIDA et les Hépatites Virales (ANRS)/Fondation de France and a grant from the European Community (Marie Curie International Reintegration Grant, FP6).

(FF) was supported by a grant from ANR (Agence Nationale de la Recherche, France).

(SML) was supported by a grant from NIH.NIAID U19-AI40035

We thank the Center for Exploration and Experimental Functional Research (Genopole, Evry, France) for animal housing and care.

References:

1. 2002; *Hepatology*. 36: (5 Suppl 1) S3 - 20
2. Pawlotsky JM, Chevaliez S, McHutchison JG. 2007; *Gastroenterology*. 132: (5) 1979 - 1998
3. Serfaty L, Andreani T, Giral P, Carbonell N, Chazouilleres O, Poupon R. 2001; *J Hepatol*. 34: (3) 428 - 434
4. Siagris D, Christofidou M, Theocharis GJ, Pagoni N, Papadimitriou C, Lekkou A, Thomopoulos K, Starakis I, Tsamandas AC, Labropoulou-Karatzas C. 2006; *Journal of viral hepatitis*. 13: (1) 56 - 61
5. Tada S, Saito H, Ebinuma H, Ojiro K, Yamagishi Y, Kumagai N, Inagaki Y, Masuda T, Nishida J, Takahashi M, Nagata H, Hibi T. 2008; *Hepatology Res*.
6. Bach N, Thung SN, Schaffner F. 1992; *Hepatology*. 15: (4) 572 - 577
7. Castera L, Hezode C, Roudot-Thoraval F, Bastie A, Zafrani ES, Pawlotsky JM, Dhumeaux D. 2003; *Gut*. 52: (2) 288 - 292
8. Serfaty L, Mathurin P, Cadranel JF, Tran A. 2007; *Gastroenterol Clin Biol*. 31: (8-9 Pt 3) 4S40 - 43
9. Castera L, Chouteau P, Hezode C, Zafrani ES, Dhumeaux D, Pawlotsky JM. 2005; *The American journal of gastroenterology*. 100: (3) 711 - 715
10. Hezode C, Roudot-Thoraval F, Zafrani ES, Dhumeaux D, Pawlotsky JM. 2004; *Journal of viral hepatitis*. 11: (5) 455 - 458
11. Boulant S, Targett-Adams P, McLauchlan J. 2007; *The Journal of general virology*. 88: (Pt 8) 2204 - 2213
12. Miyazaki Y, Atsuzawa K, Usuda N, Watashi K, Hishiki T, Zayas M, Bartenschlager R, Wakita T, Hijikata M, Shimotohno K. 2007; *Nature cell biology*. 9: (9) 1089 - 1097
13. Shavinskaya A, Boulant S, Penin F, McLauchlan J, Bartenschlager R. 2007; *J Biol Chem*. 282: (51) 37158 - 37169
14. Appel N, Zayas M, Miller S, Krijnse-Locker J, Schaller T, Friebe P, Kallis S, Engel U, Bartenschlager R. 2008; *PLoS pathogens*. 4: (3) e1000035 -
15. Piodi A, Chouteau P, Lerat H, Hezode C, Pawlotsky JM. 2008; *Hepatology*. 48: (1) 16 - 27
16. Lerat H, Honda M, Beard MR, Loesch K, Sun J, Yang Y, Okuda M, Gosert R, Xiao SY, Weinman SA, Lemon SM. 2002; *Gastroenterology*. 122: (2) 352 - 365
17. Perlemuter G, Sabile A, Letteron P, Vona G, Topilco A, Chretien Y, Koike K, Pessayre D, Chapman J, Barba G, Brechot C. 2002; *Faseb J*. 16: (2) 185 - 194
18. Hegarty BD, Bobard A, Hainault I, Ferre P, Bossard P, Foufelle F. 2005; *Proceedings of the National Academy of Sciences of the United States of America*. 102: (3) 791 - 796
19. Blake WL, Ulrich RG, Marotti KR, Melchior GW. 1994; *Biochemical and biophysical research communications*. 205: (2) 1257 - 1263
20. Petit JM, Benichou M, Duvillard L, Jooste V, Bour JB, Minello A, Verges B, Brun JM, Gamber P, Hillon P. 2003; *The American journal of gastroenterology*. 98: (5) 1150 - 1154
21. Kumar D, Farrell GC, Fung C, George J. 2002; *Hepatology*. 36: (5) 1266 - 1272
22. Negro F. 2002; *Hepatology*. 36: (5) 1050 - 1052
23. Poynard T, Ratziu V, McHutchison J, Manns M, Goodman Z, Zeuzem S, Younossi Z, Albrecht J. 2003; *Hepatology*. 38: (1) 75 - 85
24. Rubbia-Brandt L, Giostra E, Mentha G, Quadri R, Negro F. 2001; *J Hepatol*. 35: (2) 307 -
25. Baiocchi L, Tisone G, Palmieri G, Rapicetta M, Pisani F, Orlando G, Casciani CU, Angelico M. 1998; *Liver Transpl Surg*. 4: (6) 441 - 447
26. Keasler VV, Lerat H, Madden CR, Finegold MJ, McGarvey MJ, Mohammed EM, Forbes SJ, Lemon SM, Hadsell DL, Grona SJ, Hollinger FB, Slagle BL. 2006; *Virology*. 347: (2) 466 - 475
27. Disson O, Haouzi D, Desagher S, Loesch K, Hahne M, Kremer EJ, Jacquet C, Lemon SM, Hibner U, Lerat H. 2004; *Gastroenterology*. 126: (3) 859 - 872
28. Erdtmann L, Franck N, Lerat H, Le Seyec J, Gilot D, Cannie I, Gripon P, Hibner U, Guguen-Guillouzo C. 2003; *J Biol Chem*. 278: (20) 18256 - 18264
29. Gerber MA. 1997; *Clinics in liver disease*. 1: (3) 529 - 541 vi -
30. Dai CY, Chuang WL, Ho CK, Hsieh MY, Huang JF, Lee LP, Hou NJ, Lin ZY, Chen SC, Hsieh MY, Wang LY, Tsai JF, Chang WY, Yu ML. 2008; *J Hepatol*. 49: (1) 9 - 16
31. Jackel-Cram C, Babiuk LA, Liu Q. 2007; *J Hepatol*. 46: (6) 999 - 1008
32. Yang W, Hood BL, Chadwick SL, Liu S, Watkins SC, Luo G, Conrads TP, Wang T. 2008; *Hepatology*. 48: (5) 1396 - 1403
33. Horton JD, Goldstein DJ, Brown MS. 2002; *The Journal of clinical investigation*. 109: (9) 1125 - 1131
34. Waris G, Felmlee DJ, Negro F, Siddiqui A. 2007; *Journal of virology*. 81: (15) 8122 - 8130
35. McPherson S, Jonsson JR, Barrie HD, O'Rourke P, Clouston AD, Powell EE. 2008; *J Hepatol*. 49: (6) 1046 - 1054
36. Kim KH, Hong SP, Kim K, Park MJ, Kim KJ, Cheong J. 2007; *Biochemical and biophysical research communications*. 355: (4) 883 - 888
37. Oem JK, Jackel-Cram C, Li YP, Zhou Y, Zhong J, Shimano H, Babiuk LA, Liu Q. 2008; *The Journal of general virology*. 89: (Pt 5) 1225 - 1230
38. Ishii S, Iizuka K, Miller BC, Uyeda K. 2004; *Proceedings of the National Academy of Sciences of the United States of America*. 101: (44) 15597 - 15604
39. Sato R, Miyamoto W, Inoue J, Terada T, Imanaka T, Maeda M. 1999; *J Biol Chem*. 274: (35) 24714 - 24720

- 40 . Mirandola S , Realdon S , Iqbal J , Gerotto M , Dal Pero F , Bortoletto G , Marcolongo M , Vario A , Datz C , Hussain MM , Alberti A . 2006 ; Gastroenterology . 130 : (6) 1661 - 1669
- 41 . Domitrovich AM , Felmlee DJ , Siddiqui A . 2005 ; J Biol Chem . 280 : (48) 39802 - 39808
- 42 . Choukhi A , Ung S , Wychowski C , Dubuisson J . 1998 ; Journal of virology . 72 : (5) 3851 - 3858
- 43 . Tardif KD , Mori K , Siddiqui A . 2002 ; Journal of virology . 76 : (15) 7453 - 7459
- 44 . Pavo N , Romano PR , Graczyk TM , Feinstone SM , Taylor DR . 2003 ; Journal of virology . 77 : (6) 3578 - 3585

Fig. 1

Histological sections of paraffin-embedded livers from wild-type (A) and HCV transgenic mice (B and C). (A) Hematoxylin-eosin staining of non transgenic liver. (B) Hematoxylin-eosin staining of transgenic liver showing microvesicular steatosis characterized by small vacuoles in the cytoplasm of hepatocytes surrounding the central vein area. (C) Oil-red-O staining of transgenic liver showing the presence of neutral lipids (red dots) within the hepatocyte cytoplasm.

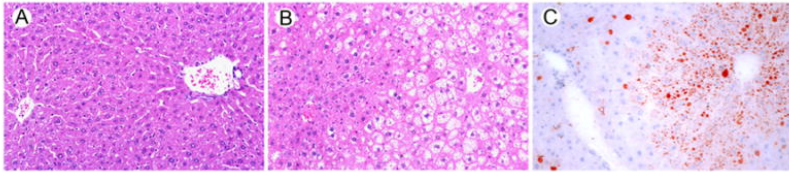
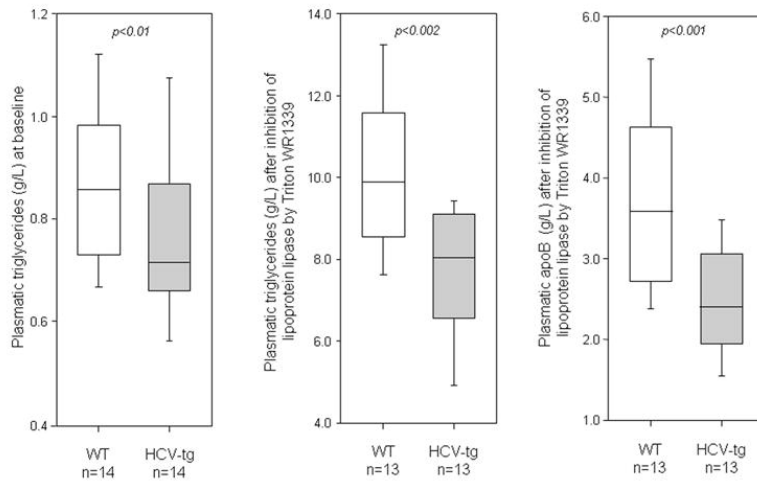


Fig. 2

(A) Hepatic secretion of VLDL, based on plasma triglyceride levels in fasted wild-type males (WT) and HCV transgenic age-matched male littermates (HCV-tg) at baseline (left) and after lipoprotein lipase inhibition by Triton WR 1339 (middle); and plasma levels of apoB after Triton WR 1339 treatment (right). (B) Microsomal transfer protein (MTP) activity in crude liver extracts from WT and HCV-tg mice. Box-and-whisker graphs are used; the line in the middle is the median, the box extends from the 25th to the 75th percentile, and the whiskers extend to the lowest and highest values. Values in WT and HCV-tg mice were compared with the Mann and Whitney test.

A



B

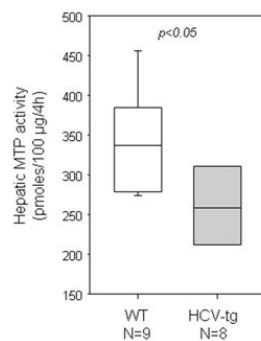


Fig. 3

(A) Gene expression of ATP citrate-lyase (ACL), acetyl-CoA carboxylase (ACC), fatty acid synthase (FAS), malic enzyme (ME) and hepatic stearoyl-CoA desaturase 1 (SCD1), assessed by RT-qPCR in the livers of wild-type mice (WT) and HCV transgenic (HCV-tg) littermates (all males, 8 to 9 months old). The results were normalized to the mean expression level in WT liver. (B) Fatty acid synthase (FAS) protein expression, assessed by western blotting. The left-hand panel shows a representative blot. Variations between samples were normalized on the basis of GAPDH expression. The results were normalized to the mean expression level in WT liver. Box-and-whisker graphs are used. Values in WT and HCV-tg mice were compared with the Mann and Whitney test.

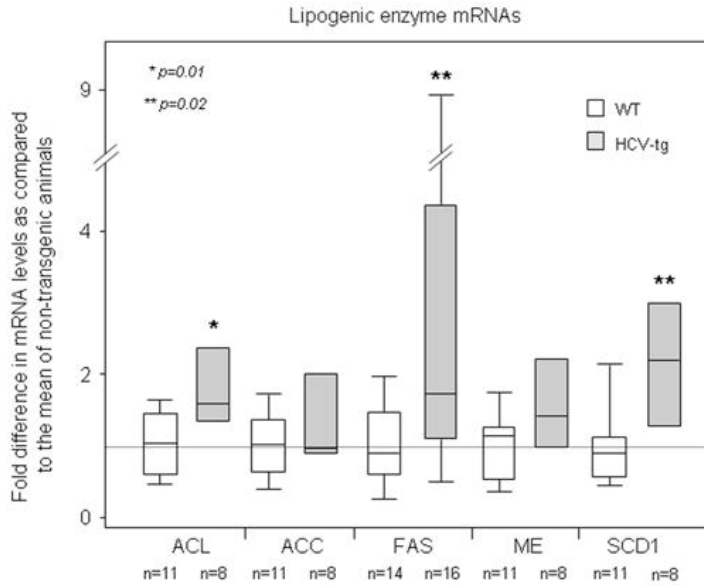
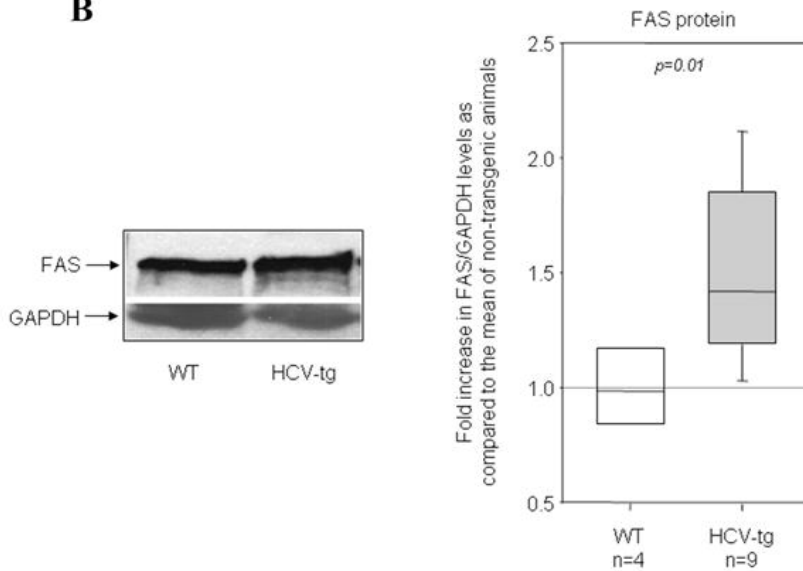
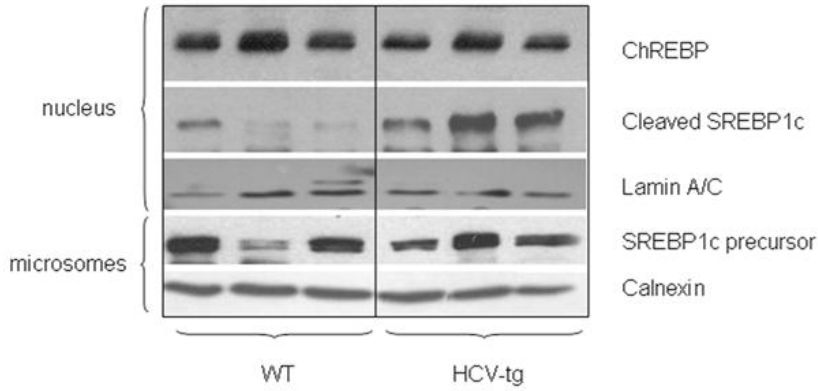
A**B**

Fig. 4

(A) Western blot analysis showing cleaved SREBP1c and nuclear ChREBP expression in wild-type mice (WT) and HCV transgenic littermates (HCV-tg); liver cell nuclear extracts are shown at the top, and liver cell microsomes extracts at the bottom. Lamin A/C and actin, respectively, were used as references. **(B)** SREBP1c and ChREBP mRNA levels assessed by RT-qPCR in the liver of WT and HCV-tg mice. The results were normalized to the mean expression level in WT liver. Box-and-whisker graphs are used. Values in WT and HCV-tg mice were compared with the Mann and Whitney test.

A



B

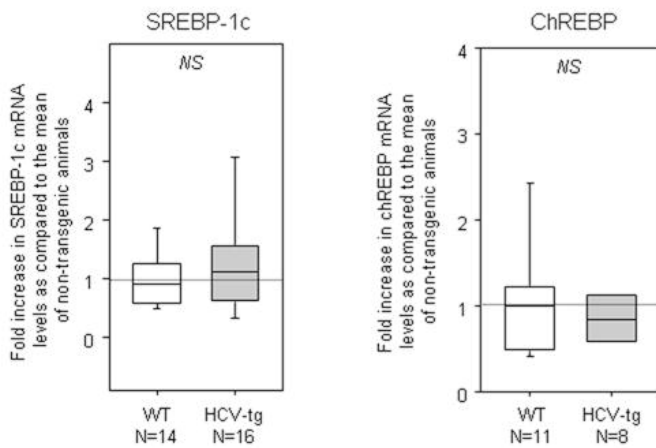
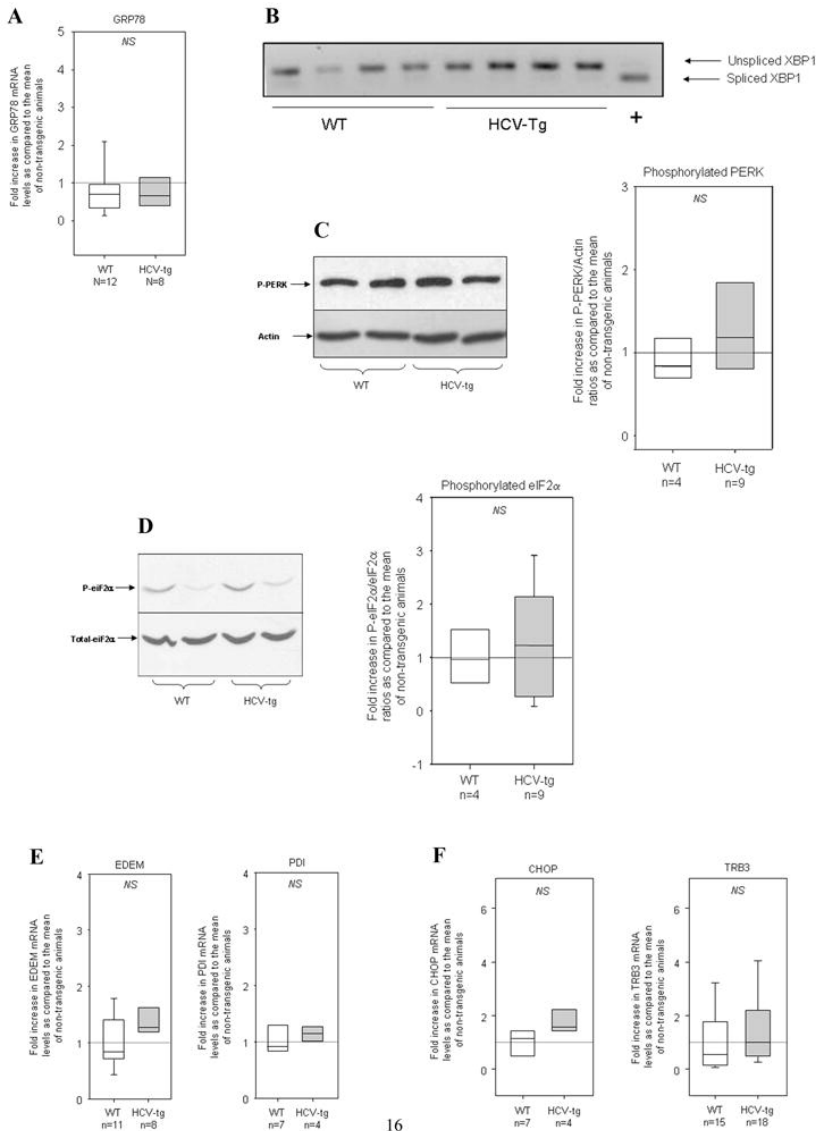


Fig. 5

(A) GRP78 mRNA levels assessed by RT-qPCR in the liver of wild-type mice (WT) and HCV transgenic littermates (HCV-tg). The results were normalized to the mean expression level in WT liver. Box-and-whisker graphs are used. Values in WT and HCV-tg mice were compared with the Mann and Whitney test. **(B)** Unspliced and spliced XBP1 mRNA transcripts in liver RNA extracts from WT and HCV-tg mice, as assessed by RNA size discrimination on agarose gel. A positive control (+) showing spliced XBP1 was migrated in parallel. **(C)** Respective amounts of the phosphorylated form of PERK, as assessed by western blot, in WT and HCV-tg mice. Left: representative western blot; right: box-and-whisker graphs. Values in WT and HCV-tg mice were compared with the Mann and Whitney test. **(D)** Respective amounts of the phosphorylated form of eIF2 α , as assessed by western blot, in WT and HCV-tg mice. Left: representative western blot; right, box-and-whisker graphs. Values in WT and HCV-tg mice were compared with the Mann and Whitney test. **(E)** EDEM and PDI mRNA levels assessed by RT-qPCR in the liver of WT and HCV-tg mice. The results were normalized to the mean expression level in WT liver. Box-and-whisker graphs are used. Values in WT and HCV-tg mice were compared with the Mann and Whitney test. **(F)** CHOP and TRB3 mRNA levels assessed by RT-qPCR in the liver of WT and HCV-tg mice. The results were normalized to the mean expression level in WT liver. Box-and-whisker graphs are used. Values in WT and HCV-tg mice were compared with the Mann and Whitney test.



16

Table 1

Sequences of the primers used for quantitative real-time PCR.

| | |
|-----------------|---|
| SREBP-1c | 5'-ggagccatggattgcacatt-3' 5'-ggcccgggaagtcactgt-3' |
| ChREBP | 5'-gtccgatatctccgacacacttt-3' 5'-cattgccaacataagcgtcttctg-3' |
| FAS | 5'-tgctcccagctgcaggc-3' 5'-gcccggtagctctgggtga-3' |
| SCD1 | 5'-acctgcctctcgggattt-3' 5'-gtcggcgtgtttctgaga-3' |
| ME | 5'-gggcatccctgtggtaaa-3' 5'-gaaggcgtcatactcagggc-3' |
| ACL | 5'-ctccaaactgaccgcca-3' 5'-ggagtgtcctggtagcgag-3' |
| ACC | 5'-tgggcacagaccgtgtag-3' 5'-gtcttaaatgcagagtctggaa-3' |
| GRP78 | 5'-gaaaggatggttaatgatgctgag-3' 5'-gtcttcaatgcccatcctg-3' |
| TRB3 | 5'-ctctgaggctccaggacaag-3' 5'-ggctcaggctcatctctcac-3' |
| EDEM | 5'-ggatcccctatccctcgggt-3' 5'-gttgctccgaagtccag-3' |
| CHOP | 5'-catacaccaccacctgaaag-3' 5'-ccgttctctagttcttcttc-3' |
| PDI | 5'-aacgggagaagccattgta-3' 5'-aggtgtcatccgctcagctct-3' |